Nuclear Instruments and Methods in Physics Research B 86 (1994) 12–19
North-Holland

NIM B
Beam Interactions with Materials & Atoms

Alignment and orientation in atomic collisions

C.D. Lin [a,*], N. Toshima [b] and W. Fritsch [c]

[a] *Department of Physics, Kansas State University, Manhattan, Kansas, USA*
[b] *Institute of Applied Physics, University of Tsukuba, Tsukuba, Ibaraki 350, Japan*
[c] *Hahn–Meitner Institute Berlin GmbH, D-1000 Berlin, Germany*

Recent experimental and theoretical studies of alignment, orientation and dipole moments of excited states formed in atomic collisions for simple systems are reviewed. We also review the studies of the dependence of electron capture cross sections on the magnetic quantum numbers of the initial target states. The propensity rule involving the magnetic quantum numbers in atomic collisions is also examined.

1. Introduction

In a quantum-mechanical description of inelastic ion-atom collisions, the time evolution of the final electronic state of either collision partner at the end of the collision can be represented as a coherent sum of atomic eigenstates ϕ_i

$$\psi(t > t_0) = \sum_i a_i(t_0)\phi_i \exp^{(-i\epsilon_i t)}, \quad (1)$$

where the expansion coefficient a_i is proportional to the scattering amplitude for populating the excited state ϕ_i from a well-defined initial state, and time t_0 is supposed to be large enough to ensure that couplings among the final states have vanished. In experiments where the total cross sections are measured, only the magnitudes of the scattering amplitudes a_i are explored. In the so-called coherence and correlation studies, one of the goals is to find the phase information on these scattering amplitudes.

The wave function represented by Eq. (1) is actually a decaying pure state. Since experimental observation takes some finite time interval, coherence can be observed only among states which are degenerate or near degenerate. In this review we will concentrate only on the coherence among states which are degenerate. Thus the alignment and orientation studies pertain to the investigations of the relative magnitudes and phases of the amplitudes among the magnetic substates of a given nl subshell. In the case of hydrogenic excited states, the degeneracy among the subshell states for a given principal quantum number n also allows the study of coherence among substates of different angular momenta.

There is a rich literature on the alternative yet equivalent theoretical formulations of "coherence and correlation" studies [1–5], see for example Andersen et al. [3]. To extract orientation and alignment parameters from experiments, the polarization or the angular distribution of the emitted photons from the radiative stablization of the excited states has to be measured. For atomic states with fine or hyperfine structures, the effect of "depolarization" of the radiation due to the fine structure and hyperfine structure has to be considered. This subject has been discussed extensively in the literature (see refs. [1–4]). When the collision involves the excitation of inner shells or of multiply excited states, decay by electron emission is possible and the orientation and alignment can also be studied by measuring the angular distribution of the ejected electron.

We will concentrate only on simple collision systems, especially those where both experiments and elaborate theoretical calculations are available. In section 2 we review briefly the different coherence parameters commonly used. Section 3 reviews examples of alignment and orientation studies for excited states formed by collisions with simple atoms in the ground state. Section 4 is devoted to collisions with laser-excited target atoms. While the alignment and orientation studies for specific systems are interesting, it is of paramount importance to examine if any of these parameters exhibit special simple trends or rules. In both sections 3 and 4, the possibility of these propensity rules are also examined. A short summary is given in section 5.

* Corresponding author.

SSDI 0168-583X(93)E0871-D

2. Coherence parameters

2.1. Coherence between magnetic substates

The scattering amplitudes a_i in Eq. (1) are suitable for describing pure states. An alternative approach is to describe the end of a collision event in terms of density matrix. The density matrix approach can be used to represent mixed states as well (see refs. [3,4]). We will treat pure states here only, thus the density matrix is

$$\rho_{JM,J'M'} = a_{JM} a^*_{J'M'}. \tag{2}$$

An alternative representation of the coherence parameters is to use the state multipoles which are the irreducible representations of the density matrix. There are different definitions of such multipoles, the alignment A and the orientation parameters O defined by Fano and Macek [1] are real quantities constructed from the expectation values of angular momentum operators:

$$\begin{aligned}
&\langle J_y \rangle = J(J+1)0 \\
&\langle 3J_z^2 - J^2 \rangle = J(J+1)A_{20} \\
&\langle (J_x J_z + J_z J_x) \rangle = J(J+1)A_{21} \\
&\langle \left(J_x^2 - J_y^2\right) \rangle = J(J+1)A_{22},
\end{aligned} \tag{3}$$

where the quantization axis is chosen to be along the direction of the incident beam.

2.2. Coherence between degenerate hydrogenic states

Due to the degeneracy of hydrogenic sublevels within a given principal quantum number n, the coherence among the nlm substates, represented by the density matrix $\langle nlm | \rho | nl'm' \rangle$ can be determined in principle experimentally. The decomposition of such a density matrix in terms of state multipoles where the multipoles have obvious physical interpretations has been obtained based on the O_4 group of the nonrelativisitic hydrogen atom [6]. Starting with the two constants of motion, the angular momentum $\boldsymbol{L}$ and the Runge–Lenz vector $\boldsymbol{A}$, the state multipoles thus constructed contain the Fano–Macek orientation and alignment parameters as a subset. Among them which we will discuss later are the expectation value of $\boldsymbol{A}$ and of $\boldsymbol{L} \times \boldsymbol{A}$, where $\boldsymbol{A}$ is proportional to the electric dipole moment operator D for a given n-shell, and $\boldsymbol{L} \times \boldsymbol{A}$ is proportional to the velocity vector of a classical electron at the perihelion. These expectation values can be expressed in terms of linear combinations of density matrix elements.

2.3. Coherence parameters from integral measurements

In experiments where the scattering angles of the incident particles are not determined, the collision system has cylindrical symmetry, thus only the alignment parameter A_{20} can be determined. In the simple case that the target is a closed-shell atom where the projectile and target are not polarized, and where the scattering angles or the recoil ions are not detected, the linear polarization P and the angular distribution of the emitted photon are related to A_{20} by

$$\begin{aligned}
&P = 3\alpha_2 \frac{A_{20}}{\alpha_2 A_{20} - 2} \\
&W(\theta) = W_0 [1 + \alpha_2 A_{20} P_2(\cos\theta)]/4\pi.
\end{aligned} \tag{4}$$

Here α_2 is a constant depending on the angular momentum of the initial and final states. If the excited state is a 2p (or np in general) state, then the alignment parameter A_{20} is related to the subshell cross section σ_m for populating $2p_m$ magnetic substates by

$$A_{20} = \frac{\sigma_1 - \sigma_0}{2\sigma_1 + \sigma_0}. \tag{5}$$

For hydrogenic excited states, the cylindrical symmetry allows only the determination of the z-component of $\boldsymbol{A}$ and of $\boldsymbol{L} \times \boldsymbol{A}$. These expectation values can be expressed in terms of the real and imaginary components of the density matrices as [7,8]

$$\begin{aligned}
\langle D_z \rangle_{n=2} &= \frac{6\ \mathrm{Re}(\sigma_{s,p_0})}{\sigma_{2s} + \sigma_{2p}} \\
\langle (\boldsymbol{L} \times \boldsymbol{A})_z \rangle_{n=2} &= \frac{-2\ \mathrm{Im}(\sigma_{s,p_0})}{\sigma_{2s} + \sigma_{2p}} \\
\langle D_z \rangle_{n=3} &= \frac{6\sqrt{2}\,\mathrm{Re}\left(\sigma_{s,p_0} + \sqrt{\tfrac{1}{2}}\sigma_{p_0,d_0} + \sqrt{\tfrac{3}{2}}\sigma_{p_1,d_1}\right)}{\sigma_{3s} + \sigma_{3p} + \sigma_{3d}} \\
\langle (\boldsymbol{L} \times \boldsymbol{A})_z \rangle_{n=3} &= \frac{4\sqrt{\tfrac{2}{3}}\,\mathrm{Im}\left(\sigma_{s,p_0} + \sqrt{2}\sigma_{p_0,d_0} + \sqrt{6}\sigma_{p_1,d_1}\right)}{\sigma_{3s} + \sigma_{3p} + \sigma_{3d}}.
\end{aligned} \tag{6}$$

2.4. Alternative coordinate frames

In describing an atomic collision, often the direction of the incident beam is chosen to be the z-direction, or the quantization axis where the magnetic quantum number is referred to. This choice is definite unique for integral measurements where the beam axis is the axis of the cylindrical symmetry. In the case of differential measurements, the incident beam and the scattered beam define a scattering plane. The x-axis is chosen to lie on the scattering plane with the scattered particles measured in the $+x$-direction. The y-axis is chosen to be perpendicular to the scattering plane such that x, y and z form a right-handed orthogonal set of axes. An alternative choice of the coordinate frame, called the natural frame, $x'y'z'$ (see Fig. 1), is to

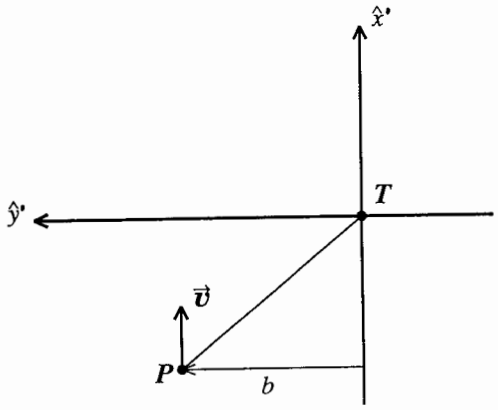

Fig. 1. The natural coordinate system for atomic collisions. The collision plane is the $x'y'$ plane, with the $+x'$ being the direction of the incident beam. The quantization axis is the $+z'$ axis which is pointing out of the paper.

choose the quantization axis along the direction perpendicular to the scattering plane, i.e. $z'=y$, and $x'=z$ and $y'=x$. The scattering amplitudes or density matrices referred to one coordinate frame can be obtained from the other by simple rotation matrices. For latter discussions, we give explicit expressions for the subspace of 2p magnetic substates. Referring to the xyz frame, the coherent 2p wave function can be expressed as

$$\psi = a_0\phi_{2p_0} + a_1\phi_{2p_1} + a_{-1}\phi_{2p_{-1}}, \tag{7}$$

from which we can define the expectation value of the angular momentum perpendicular to the scattering plane $\langle L_\perp \rangle$, called the orientation parameter,

$$\langle L_\perp \rangle = -2\sqrt{\lambda(1-\lambda)}\sin\chi, \tag{8}$$

where λ and χ are defined as

$$\lambda = \frac{|a_0|^2}{|a_0|^2 + 2|a_1|^2}, \quad \chi = \arg(a_1/a_0). \tag{9}$$

The expression (9) shows that the orientation $\langle L_\perp \rangle$ depends on the relative phase between the amplitudes for the $2p_1$ and $2p_0$ magnetic substates (the phases for $2p_1$ and $2p_{-1}$ are fixed by the reflection symmetry with respect to the scattering plane). This has been commonly used to state that the determination of the orientation parameter provides information on the relative phase between the scattering amplitudes. This is true only if the amplitudes are defined with respect to the xyz frame.

If the scattering amplitudes are defined with respect to the $x'y'z'$ frame, the wave function (7) is rewritten as

$$\psi = a'_1\phi'_{2p_1} + a'_{-1}\phi'_{2p_{-1}}, \tag{7a}$$

where we have assumed that the collision system has even reflection symmetry with respect to the scattering plane, then the orientation parameter becomes

$$\langle L_\perp \rangle = |a'_1|^2 - |a'_{-1}|^2. \tag{8a}$$

There is no phase information in the expression above. Note the similarity of this expression to the alignment defined in Eq. (5).

2.5. Atomic scattering theories

From the calculated scattering amplitudes, all quantal scattering theories can provide the full density matrix or the corresponding coherence parameters. The atomic scattering theories which account for most of the detailed couplings among all the atomic states are usually of the close-coupling varieties. In the energy domain of tens of keV's to MeV's collisions, the motion of the heavy particles can be described classically. In the close coupling method, the time-dependent electronic wave functions are expanded in terms of certain basis functions. In the atomic orbital expansion method, the basis functions are atomic states centered on each collision partner. In the molecular orbital expansion method, the basis functions are static molecular orbitals modified by some form of electron translational factors. The close-coupling method has been reviewed recently by Fritsch and Lin [9].

3. Selective examples

3.1. Integral measurements on alignment parameters

The simplest ion–atom collision system that has been exposed to many theoretical investigation is the $H^+ + H(1s)$ collision. In the 1–50 keV energy region, the total cross sections for excitation and electron capture cross sections from the various coupled channel calculations are in quite good agreement with experiments (see ref. [9]), but the magnetic substate cross sections to the 2p states can be examined only if the integral alignments are measured. Such an experiment has been carried out by Hippler et al. [10]. Their results are shown in Fig. 2 where various theoretical results are also shown [11–13]. The experiment does not separate the 2p radiation from the excitation and electron capture channels, so the weighted average alignments are compared. It is clear that the alignment is positive at low energies since it is well understood that the 2p state in this collision system is formed by the rotational coupling between the $2p\sigma$ and the $2p\pi$ molecular states, and thus at low energies, the alignment should approach its asymptotic value of 0.5. The experimental values are close to this value in the 1–7 keV region, but tend to deviate from it at lower ener-

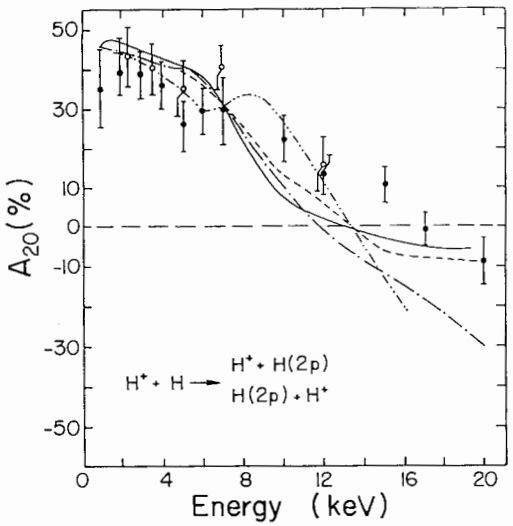

Fig. 2. Integral alignment A_{20} of H(2p) states of both target and projectile populated in $H^+ + H$ collisions. Experimental results by Hippler et al. [10] are compared with results from calculations by Fritsch and Lin [11] (dashed and dashed–dotted lines), by Shingal [12] (solid line) and by Lüdde and Dreizler [13] (dashed–double-dotted lines).

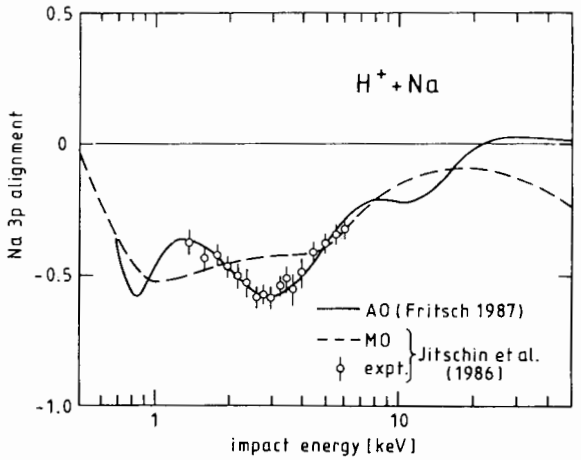

Fig. 3. Integral alignment A_{20} for $H^+ + Na(3s) \rightarrow H^+ + Na(3p)$ excitation process. Data are by Jitschin et al. [14]. Solid lines are results from the AO calculations by Fritsch [15] and dashed lines are from the smaller MO calculations [16].

gies, which may be due to the neglect in the theories in including the Coulomb deflection of the projectile trajectory at low energies. Fig. 2 also shows that there are still noticeable discrepancies between experiment and theories in the 15–20 keV collision energy region. Whether this is an indication of the failure of all the close-coupling calculations, remains to be examined.

We next show an example of the integral alignment of Na(3p) excitation produced in $H^+ + Na(3s)$ collisions. In Fig. 3 the measured alignments by Jitschin et al. [14] are compared to the AO calculations by Fritsch [15]. This system is complicated in that electron capture to the $n = 2$ states are large and many channels have to be included in the coupled-channel calculations. The smaller basis MO calculation does not give correct A_{20} in details, although the relative energy dependence is satisfactory [16]. This example gives evidence that alignment provides a more stringent test on the calculations carried out by different theoretical models.

Experimentally, the integral alignment for H(2p) in $H^+ + He \rightarrow H(2p) + He^+$ has been measured over a broad energy region, as shown in Fig. 4 [17,18]. This two-electron system poses a great challenge to the theoretical models, especially at higher energies where the capture cross sections to H(2p) are small. In Fig. 4 a number of theoretical results have been shown, and the agreement with data is not satisfactory except for the low-energy region. For more details about this system, see section 5.1.2 of Hippler [5].

There are few measurements on alignment for ion–atom collisions involving multiply charged ions. In these collisions, the electron is captured to higher exited states and polarization from the cascading radia-

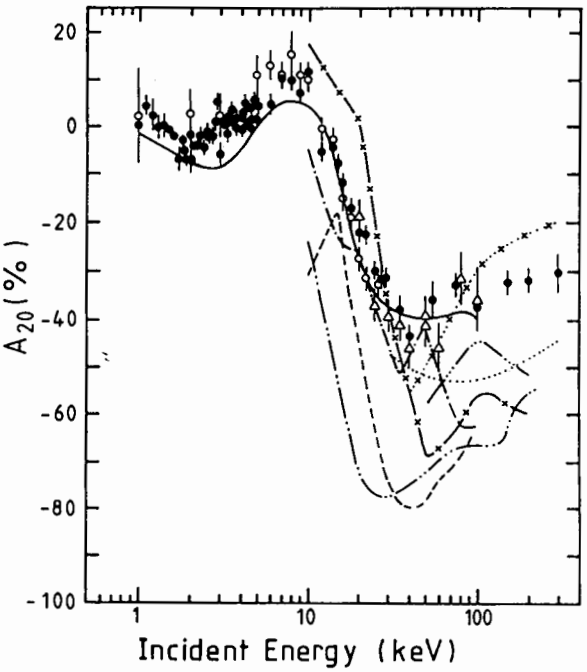

Fig. 4. Integral alignment A_{20} for capture to H(2p) in $H^+ + He$ collisions vs. incident energy. Experiment: open circles, from Teubner et al. [17]; solid circles, from Hippler et al. [18]; triangles, from Cline [19]. Theory: see the explanations in Fig. 20 of Hippler [5].

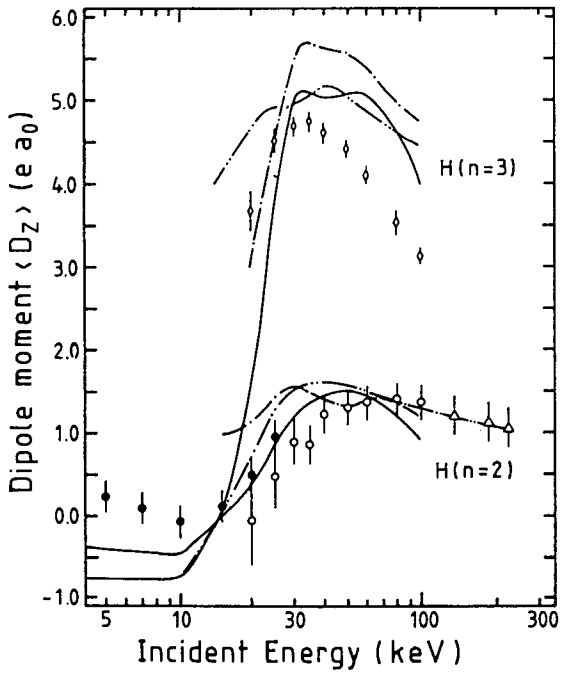

Fig. 5. Dipole moment $\langle D_z \rangle$ for electron capture to H($n = 2$) and H($n = 3$) states in $H^+ + He$ collisions vs. incident energy. Experiment: H($n = 2$), solid circles, Hippler et al. [18]; open circles, Cline [19]; triangles, DeSerio et al. [25]; H($n = 3$): diamonds, Ashburn et al. [23]. Theory: one-electron AO calculations by Shingal and Lin [26] in dashed–dotted lines; two-electron AO calculations by Slim et al. [27] in dashed–double-dotted lines and two-electron AO–MO calculations by Kimura [28] in solid lines.

tions has been measured [20]. To compare with experimental alignments, the transfer of alignment from the initial excited state has to be treated, see Lin and Macek [21].

3.2. Integral measurements on dipole moments

The coherence between the degenerate hydrogenic nl subshells can be determined partially in a number of different ways: (a) by measuring the linear polarization in an external axial and/or perpendicular electric field [22,23]; (b) by applying a radio-frequency field to drive transitions among the $n = 3$ states [24], and (c) by measuring the quantum beats in an electric field [25]. The most extensive studies have been carried out for the electron capture to the $n = 2$ and $n = 3$ manifolds in $H^+ + He$ collisions. In Fig. 5 we show the dipole moment extracted from the experiments and compare them with different theoretical calculations [7,26–28]. The general trends are predicted by these more elaborate calculations, despite that there are still some differences.

3.3. Orientation parameters

There are a few experimental studies on the orientation parameters for ion–atom collisions, but most are limited to the low-energy region, see the examples given by Hippler [5]. The small scattering angles at higher collision energies make such measurements rather difficult. On the other hand, there are a number of theoretical and some experimental evidences that there exists simple propensity rules for the orientation parameter for excited states formed in ion-atom collisions. The propensity rule was first discovered for the 2p states formed in the excitation processes [29]. Recall that in the natural frame of reference where the quantization axis is perpendicular to the scattering plane, the orientation is a measure of the different probabilities for populating the $m' = 1$ and $m' = -1$ substates. It was found that for the excitation process near the velocity matching region, the orientation parameter is near -1, indicating that the $m' = -1$ state is preferentially populated in the collision. This simple result was interpreted by Andersen and Nielsen [29] using the distorted wave approximation.

The model of Andersen and Nielsen does not apply to electron capture processes. Calculations have been carried out by Nielsen et al. [30] and there are evidences of propensity rules for electron capture processes as well. However, a clear-cut propensity rule became evident only following the work of Lundsgaard and Lin [31], where they showed that in the collisions between multiply charged ions with atoms, the dominant magnetic substates populated are the $m' = -l$ substates. In Fig. 6 the results for electron capture to 4f and 4d states in C^{6+} on H collisions at $v = 0.4$ a.u. are shown. Clearly the most negative m' values are populated and each step of increase of m' results in an order of magnitude decrease of the electron capture probability.

This propensity rule has been shown to be valid for other collision systems. The propensity rule is a consequence of the rotation of the electron cloud with the rotation of the internuclear axis throughout the collision, and is expected to be valid at higher energies and/or at larger impact parameters where the electron does not have the chance to oscillate between the two collision centers.

We conclude this section by pointing out that besides the propensity rule for the orientation parameter, there is also a general result for the dipole moment component along the direction of the incident beam for electron capture to the hydrogenic excited states [32]. Both experiment and calculations have shown that the dipole moment has positive sign in the energy region near or above the velocity matching. This implies that there is a lack of the front–back symmetry of the electron cloud after the collision – the electron

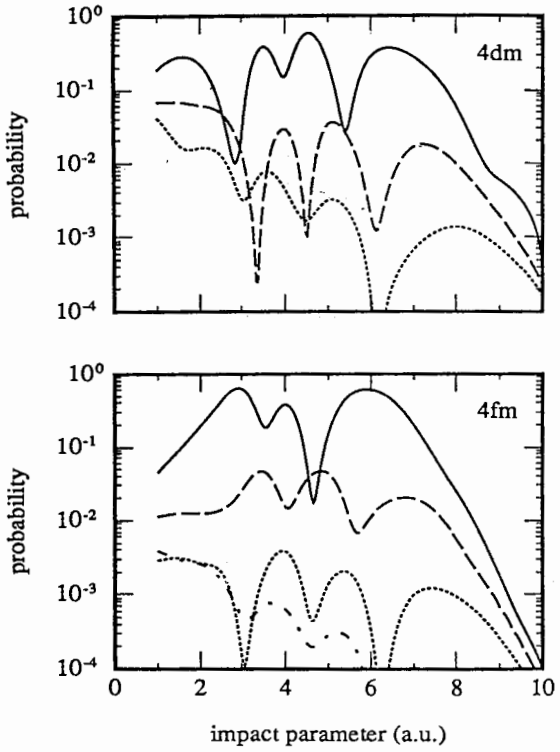

Fig. 6. The probability distributions for electron capture to 4d and 4f substates in collisions between C^{6+} on H at $v = 0.4$ a.u. [30]. The quantization axis is chosen perpendicular to the scattering plane. The magnetic quantum number $m' = -l$ has the largest probabilities, and increases in steps of 2 for each curve in order of decreasing probabilities.

cloud tends to lag behind the projectile center. This propensity rule is a consequence that the electron tends to situate between the two nuclei before the end of the collision. This interpretation implies that for excitation processes, the dipole moment tends to be negative and that the electron cloud tends to stay ahead of the target center. Close-coupling calculations for H^+ on H for excitation to $n = 2$ and $n = 3$ support this result.

4. Collisions with aligned or oriented excited states

By optical pumping techniques excited atoms can be prepared with well defined aligned or oriented states which can be served as target atoms for collisions with ions to examine the dependence of inelastic cross sections on the orbital alignment or orbital circulations. These experiments complement the analysis of polarization of final excited states examined in the previous section.

The excited states are pumped by high power lasers to achieve enough target density. Limited by the lasers available, so far all the laser excited target atoms are alkali or alkaline earth atoms. The most detailed studies have been done with the laser-excited Na(3p) states which have been produced in aligned states or in oriented states. In the study by Dowek et al. [33], the Na(3p) was aligned either parallel or perpendicular to the beam direction, and the final electron capture to the $n = 2$ and $n = 3$ states of hydrogen are determined by the energy gain/loss of the projectiles. Since only about 10% of the target atoms are in the Na(3p) states, the energy gain/loss spectra were determined with the laser on and laser off modes. By examining the spectra for the parallel and perpendicular target alignments, the dependence of electron capture cross sections of the H($n = 2$) and H($n = 3$) states on the two alignments has been determined. By defining the anisotropy $A(n)$ for electron capture to the states with principal quantum number n as the fractional difference between the cross section of the parallel aligned initial state from that of the perpendicular aligned initial state, the measured $A(n)$ is compared in Fig. 7 with the results from the theoretical calculations. The elaborate close-coupling calculations of Fritsch [34] do agree with the experimental results, but calculations with limited MO basis show discrepancy with data. Note that the anisotropy remains roughly constant for the dominant $n = 2$ electron capture channels, but changes sign for the weaker $n = 3$ channels. These results show that electron capture is more probable if

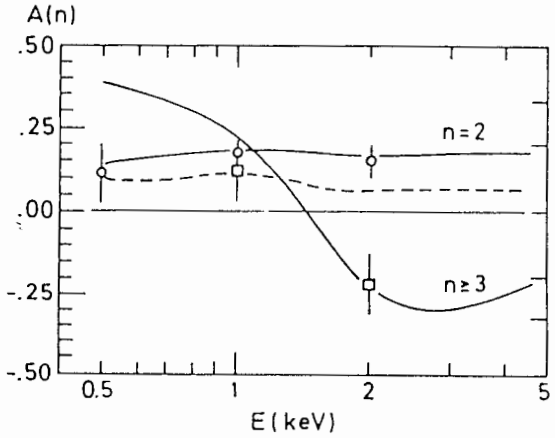

Fig. 7. The anisotropy parameter $A(n)$ as a function of incident proton energy E for electron capture to the $n = 2$ and $n = 3$ states in $H^+ + Na(3p)$ collisions. The experimental data points are from Dowek et al. [23], and the theoretical calculations in solid lines are from the AO calculations by Fritsch [34] and in dotted lines are from the MO calculations [33].

the electron cloud is aligned parallel to the incident beam direction in the collision energy range studied.

The above results for the dependence of electron capture cross sections on the initial alignment is far from universal. In fact, similar experiments [35] for collisions with He^{2+} projectiles show the opposite results: the anisotropy for the dominant $n = 4$ electron capture channel is negative and the weaker $n = 3$ channel is slightly positive, at least in the energy range of 0.5–3 keV/amu studied experimentally. The experimental results are in agreement with large-scale AO calculations carried out by Hansen, but the fact that the results are different from the collisions with protons indicate that there is no general propensity rule for the dependence of electron capture cross sections on the initial alignment of the target. Recall that there are no propensity rules for the alignments of final states in ion–atom collisions either.

The dependence of electron capture cross sections on the initial orientation of the excited target atom has been measured more recently [36]. In these experiments, the target Na(3p) atoms are prepared by using either left- or right-circularly polarized laser lights. For each polarization, the electron capture cross sections at a given scattering angle θ are measured at the left and the right of the beam. From the left–right asymmetry the dependence of the electron capture cross sections with the initial orientation can be extracted.

The comparison of experimental asymmetry parameters with theoretical calculations turns out to be not very straightforward and a simple intuitive classical model does not apply [37–39]. For $H^+ + Na(3p)$ collisions, electron capture occurs at very large impact parameters and thus corresponds to very small scattering angles. At such small angles, it is not possible to make a one–to–one correspondence between the scattering angle and the impact parameter. Using the eikonal approximation, it is possible to derive a diffraction integral which relates the scattering amplitude at a given direction (θ, ϕ) in terms of the electron capture amplitude at impact parameter b, see ref. [39]. The diffraction integral mixes amplitudes from different impact parameters and the propensity rule established for each impact parameter cannot be tested directly.

To show that at each impact parameter the electron capture probabilities do depend strongly on the initial magnetic quantum number m', we show in Fig. 8 the total electron capture probabilities vs impact parameters for different initial magnetic quantum number m' for $H^+ + H(4fm') \rightarrow H\,(all) + H^+$ collisions [40]. Note that the electron capture probabilities drop rapidly with increasing m' and that electron capture from large positive m' is less likely except at small impact parameters. Also note that if an electron is initially in the negative m' state, in the classical sense, the electron rotates in the same sense as the rotation of the internuclear axis during the collision. Such an electron is more easily captured. If the electron rotates initially opposite to the rotation of the internuclear axis, it is less likely to be captured. The results of Fig. 8 are consistent with this simple picture.

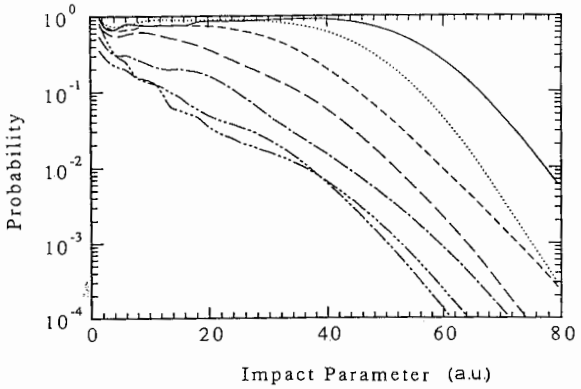

Fig. 8. Comparison of the total electron capture probabilities vs. impact parameter for different initial m' for $H^+ + H(4fm') \rightarrow H(total) + H^+$ collisions at $v = 0.2$ a.u. The solid line is for $m' = -3$, and the other lines, in order of decreasing probabilities, are $m' = -2, -1, 0$.

There are few data on electron capture from excited target atoms using multiply charged ions. Total electron capture cross sections for Ar^{7+} colliding with Na(3p) atoms have been measured by Walch et al. [41]. They also found no significant dependence of electron capture cross sections on the alignment of the excited Na(3p) states.

5. Summary

Measurements of the alignment and orientation parameters provide detailed information on the collision dynamics which are otherwise not available from measurements of total cross sections alone. These measurements, especially at the differential level, are quite tedious and time consuming, yet they are indispensable for a full understanding of the collision system and serve to distinguish the validity of different theoretical models. On the other hand, these measurements should be complemented by total and partial cross section measurements to different excited states, thus providing a full test of all the quantities calculated by the theoretical models.

The number of collision systems where orientation and alignment parameters that have been measured is still quite limited. Given the complexities of these measurements, efforts should be directed toward a few simple systems where the corresponding theoretical effort is possible. In this respect, collisions involving quasi-one electron systems are the most suitable. The

possibility of doing these studies using oriented and/or aligned excited states also add many opportunities in this field.

Acknowledgements

This work is supported in part (C.D.L.) by the US Department of Energy, Office of Basic Energy Sciences, Division of Chemical Sciences. N.T. and C.D.L. are also supported in part by the US–Japan Cooperative Research Program.

References

[1] U. Fano and J.H. Macek, Rev. Mod. Phys. 45 (1973) 553.
[2] K. Blum, Density Matrix Theory and Applications (Plenum, New York, 1982).
[3] N. Andersen, J.W. Gallagher and I.V. Hertel, Phys. Rep. 165 (1988) 1.
[4] J. Burgdörfer, in: Fundamental Processes of Atomic Dynamics, eds. J. Briggs, H. Kleinpoppen and H. Lutz (Plenum, New York, 1988).
[5] R. Hippler, J. Phys. B 26 (1993) 1.
[6] J. Burgdorfer, Z. Phys. A 309 (1983) 285.
[7] R. Shingal and C.D. Lin, unpublished (1989).
[8] A. Jain, C.D. Lin and W. Fritsch, Phys. Rev. A 36 (1987) 2041.
[9] W. Fritsch and C.D. Lin, Phys. Rep. 202 (1991) 1.
[10] R. Hippler, H. Madeheim, W. Harbich, H. Kleinpoppen and H.O. Lutz, Phys. Rev. A 38 (1988) 1662.
[11] W. Fritsch and C.D. Lin, Phys. Rev. A 26 (1982) 762; A 27 (1983) 3361.
[12] R. Shingal, private communication.
[13] H.J. Lüdde and R.M. Dreizler, J. Phys. B 15 (1982) 2703.
[14] W. Jitschin, S. Osimitsch, D.W. Mueller, H. Reihl, R.J. Allan, O. Schöller and H. Lutz, J. Phys. B 19 (1986) 2299.
[15] W. Fritsch, Phys. Rev. A 35 (1987) 2342.
[16] See the calculations in ref. [14].
[17] P.J.O. Teubner, W.E. Kaupilla, W.L. Fite and R.J. Girnius, Phys. Rev. A 2 (1970) 1763.
[18] R. Hippler, O. Plotzke, W. Harbich, H. Madeheim, H. Kleinpoppen and H.O. Lutz, Z. Phys. D 18 (1991) 61; Phys. Rev. A 43 (1991) 2587.
[19] R. Cline, Ph.D. thesis, University of North Carolina, 1991.
[20] L.J. Lemo et al., Phys. Rev. A 37 (1988) 1141.
[21] C.D. Lin and J.H. Macek, Phys. Rev. A 35 (1987) 5005.
[22] C.C. Havener, N. Rouze, W.B. Westerveld and J.S. Risley, Phys. Rev. A 33 (1986) 276.
[23] J.R. Ashburn, R.A. Cline, C.D. Stone, P.J.M. van der Burgt, W.B. Westerveld and J.S. Risley, Phys. Rev. A 40 (1989) 4885.
[24] M.C. Brower and F.M. Pipkin, Phys. Rev. A 39 (1989) 3323.
[25] R. DeSerio et al., Phys. Rev. A 37 (1988) 4111.
[26] R. Shingal and C.D. Lin, J. Phys. B 24 (1991) 963.
[27] H.A. Slim, E.L. Heck, B.H. Bransden and D.R. Flower, J. Phys. B 24 (1991) 1683.
[28] M. Kimura, Phys. Rev. A 44 (1991) R5339.
[29] N. Andersen and S.E. Nielsen, Z. Phys. D 5 (1987) 309.
[30] S.E. Nielsen, J.P. Hansen and A. Dubois, J. Phys. B 23 (1990) 2595.
[31] M.F.V. Lundsgaard and C.D. Lin, J. Phys. B 25 (1992) L429.
[32] See section 5.3 of ref. [9].
[33] D. Dowek, J.C. Houver, J. Pommier, C. Richter, T. Royeer, N. Andersen and B. Palsdottir, Phys. Rev. Lett. 64 (1990) 1713.
[34] W. Fritsch, Phys. Rev. A 35 (1987) 2342.
[35] F. Aumayr, M. Gieler, J. Schweiner, H. Winter and J.P. Hansen, Phys. Rev. Lett. 68 (1992) 3277.
[36] J.C. Houver, D. Dowek, C. Richter and N. Andersen, Phys. Rev. Lett. 68 (1992) 162.
[37] A. Dubois, S.E. Nielsen and J.P. Hansen, J. Phys. B 26 (1993) 705.
[38] C. Richter, N. Andersen, J.C. Brenot, D. Dowek, J.C. Houver, J. Salgado and J.W. Thomsen, J. Phys. B 26 (1993) 723.
[39] J.P. Hansen, S.E. Nielsen and A. Dubois, Phys. Rev. A 46 (1992) R5331.
[40] N. Toshima and C.D. Lin, Phys. Rev. A, to be published.
[41] B. Walch, S. Maleki, R. Ali, M. Stockli, M. Raphaeliaan, C.L. Cocke and B.D. Depaola, Phys. Rev. A 47 (1993) R3499.